

## Influence of PTFE on water transport in gas diffusion layer of polymer electrolyte membrane fuel cell

Yanan Chen<sup>1</sup>, Tian Tian<sup>1</sup>, Zhaohui Wan<sup>1, 2</sup>, Fan Wu<sup>1</sup>, Jinting Tan<sup>1,\*</sup>, Mu Pan<sup>1,\*</sup>

<sup>1</sup> Hubei Key Laboratory of Fuel Cells, State Key Laboratory of Advanced Technology for Materials Synthesis and Processing, 430070, Wuhan China;

<sup>2</sup> Wuhan WUT New Energy Co., Ltd, 430223, Wuhan China

\*E-mail: [tanjinting@whut.edu.cn](mailto:tanjinting@whut.edu.cn), [panmu@whut.edu.cn](mailto:panmu@whut.edu.cn)

Received: 21 December 2017 / Accepted: 10 February 2018 / Published: 6 March 2018

---

Hydrophobic coatings (PTFE) have been introduced in gas diffusion layers to improve the performance of fuel cells. Eight different cell configurations with various PTFE loading in cathode and anode GDLs were assembled. The oxygen transport ability and the water behavior are investigated based on the limiting current theory. The results demonstrate that fuel cell with a PTFE loading in GDL of 10 wt. % has the best performance of  $1.003 \text{ W}\cdot\text{cm}^{-2}$  under  $1686.6 \text{ mA}\cdot\text{cm}^{-2}$ . The high operating temperature ( $\geq 60 \text{ }^\circ\text{C}$ ) will be properly applied to characterize the oxygen transport through limiting current method. Moreover, the content of PTFE in GDL used in anode will affect the water behaviors of cathode CLs which will determine the  $R_{\text{NP}}$  in corresponding cathode, especially low Pt loading.

---

**Keywords:** PEMFC, PTFE, GDL, limiting current, oxygen transport, water behavior

### 1. INTRODUCTION

Polymer electrolyte membrane fuel cells (PEMFCs) are regarded as a promising alternative clean energy for automobiles. Cost are still considered to be the critical issues that hinder the commercialization of fuel cell vehicles. Pt is a precious metal occupying a substantial portion of the total cost of PEMFCs, reduction of the total amounts of Pt is essential for cost reduction of Fuel Cell Electric Vehicles (FCEVs) [1]. From this point, operating under higher current density with lower Pt loading is the effective way since it contributes to reduce both the amount of catalysts and the weight of stacks. Operating under higher current density, however, consumed oxygen by electrochemical reaction in catalyst layer (CL) enlarges resulting in a severe voltage drop. Therefore, liquid water will accumulate in gas diffusion layers (GDLs) or CLs which blocks the passage of oxygen and increases

the risk of voltage drop of cells. Therefore, in order to realize the high current density operation, it is necessary to reduce the oxygen transport loss and improve the water management.

In GDLs, liquid water is transferred from the CLs to flow channels by capillary forces [2]. In the opposite direction, the electrode surface requires an effective diffusion of reactant gas to maintain the polarization loss of the oxygen reduction reaction (ORR). GDL is the transport medium of this concurrent two-phase flow and its hydrophilicity, porosity, tortuosity and even the thermal conductivity will affect the coordination of this process [3, 4]. Polytetrafluoroethylene (PTFE) as the popular hydrophobic coating on GDLs can affect the oxygen flux and water behaviors through modifying the structure of the carbon paper or cloth [5], which increases water contact angle and capillary pressure [6, 7].

Various researchers have investigated the influence of hydrophobic coatings on GDLs with ex-situ and in-situ techniques [2-4, 8-20]. Ex-situ study performed with Scanning Electron Microscopy (SEM) and neutron imaging have shown that hydrophobic coatings had an important impact on the pore structure of the GDLs [3]. Lim et al [2] reported that the fluorinated ethylene propylene (FEP) coating preferentially accumulated at multiple intersecting graphite's fibers during the application process, which may block the pores under certain conditions. A detailed study of the change of the pore size distribution had been performed by Park et al [21] with mercury intrusion measurements. Prasanna et al [22] showed that the air permeability would lower with the high load coating in dry GDLs. Water penetration measurements also showed that higher coating loading led to an increase in capillary pressure threshold [23]. Ismail et al [15] considered that a decrease in average pore size not only reduced permeability but also increased permeability. LaManna and Kandlikar found that high coating loading led to high tortuosity which resulted in increasing the three-dimensional diffusion path of water vapor [24]. Gostick et al [18] performed capillary pressure measurements with different liquids (e.g. mercury, water, and octane). Based on these measurements, it was inferred that an excess PTFE coating resulted in an increase in coating thickness without increasing the covered fraction of carbon fibers. Lobato et al [25] concluded that a 10 wt. % PTFE coating had resulted in a graphite fiber coverage of 97.3% through SEM observations. This finding is consistent to report of Lim et al [2]. However, only Toray carbon papers had been investigated and no other state-of-the-art GDL materials information could be found.

Many researchers have studied the effect of PTFE coatings on membrane electrode assembly (MEA) performance by single fuel cell testing. Various coating contents has been reported in literatures, such as 5wt.% [3, 14], 10wt.% [2], 20-23 wt.% [4, 17, 22], or even 30 wt.% [17]. However, GDLs without MPL or non-of-the-art membranes were used in most of cases [2, 14, 21, 23, 26, 27]. Consequently, most reported results had the very low performance and it was very difficult to operate under current density up to  $1 \text{ A}\cdot\text{cm}^{-2}$ . Obviously, it is far away to the new requirement ( $1.5 \text{ A}\cdot\text{cm}^{-2}$ ) put forward by The U.S. Department of Energy (DOE) [28]. Most of the studies were conducted in the lab-scale ( $25\text{-}50\text{cm}^2$ ), and less studies were in small size [2, 12, 14, 21, 23, 26, 27]. Lin et al [19] studied an interdigitated flow field fuel cell with an area of  $6 \text{ cm}^2$  using technical stoichiometry (Below 5), which induced major changes in the gas and water transport mechanisms. Mukundan et al [29] performed in-plane neutron radiography measurements on a  $2.25\text{cm}^2$  small-scale cell. In order to be able to compare the experimental results with a technical fuel cell with an effective area of  $50 \text{ cm}^2$ ,

they used a flow field with a single serpentine in their experiments, which resulted in similar channel lengths and gas velocities. The commercial GDL materials of SGL series 24 with 5 and 20% PTFE were used to study the influence of the water distribution on the performance. However, the authors have not yet conducted any further analysis on the accumulation and distribution of water in the two materials. The study concluded that the amount of hydrophobic coating in a microporous layer (MPL) is critical to efficient water removal. The influence of hydrophobic coating of GDLs has been investigated by various experiments, and different explanations have been given. An agreement can be found that uncoated GDLs tend to show a high risk of flooding in the GDL [20, 30]. In contrast, the explanation about the water transport inside highly PTFE coated GDLs is very different in literature. According to Park et al [21] high coated GDLs are prone to suffer flooding in the CLs. This find can be related to the fact that MPL had not been used in their experiments. Lim et al [2] explained the poor performance at high coating was due to the diffusion resistance of the reactant gases. Recently, Biesdorf and Forner-Cuenca had systematically studied the hydrophobic coating on GDLs and developed the novel GDLs with patterned wettability which had the better performance [3, 31-34]. They presented that the amount of PTFE in the GDL had less impact on flooding the MPL and the CL. Moreover, the mass transport loss was primarily relative to the water distribution and the accumulation of water in cells. However, the synthetic method of the FEP patterned coated GDLs is complicated and lead to a high cost of GDL.

More studies only use I-V curves and impedance spectroscopy to study their fuel cell rather than more specific methods such as pressure drop analysis [19], neutron radiography [29] and limiting current method [3, 14]. Caulk and Baker studied the water transport in hydrophobic GDL by limiting current method [35-37] and they reported that there were three regions in the GDLs dry region, transition region and wet region respectively. The saturated situation in GDLs was mainly regarded for evaluating the water management ability in PEMFC [38]. However, only Toray series carbon papers were released in their work.

In this paper, we have studied the influence of content of PTFE coating in GDLs of PEMFC on performance by limiting current method. Different operating parameters such as temperatures, pressure effect have been investigated. The oxygen transport and water behaviors were analyzed through the oxygen transport resistance measurement results. We have provided a further understanding of the ongoing processing inside the GDL according these results.

## 2. EXPERIMENTS

### 2.1 The GDLs and the preparation of MEAs

The MEAs with different contents of PTFE (0 wt. %, 10 wt. %, 20 wt. % and 30 wt. %, respectively) in GDLs were purchased from Wuhan New Energy Co., Ltd. Each active area of MEAs was 4 cm<sup>2</sup>, and the PEM was Nafion XL thin film. And the Pt loading of MEAs in the anode and cathode CLs were 0.1 mg·cm<sup>-2</sup> and 0.4 mg·cm<sup>-2</sup>, respectively.

2.2 Characterization of GDLs

The pore size distribution of GDLs was measured using mercury intrusion porosimetry conducted on autopore9500. Surface images of the GDLs were taken by field-emission scanning electron microscope (FESEM, Nova NanoSEM 450).

2.3 Fuel cell measurement setup

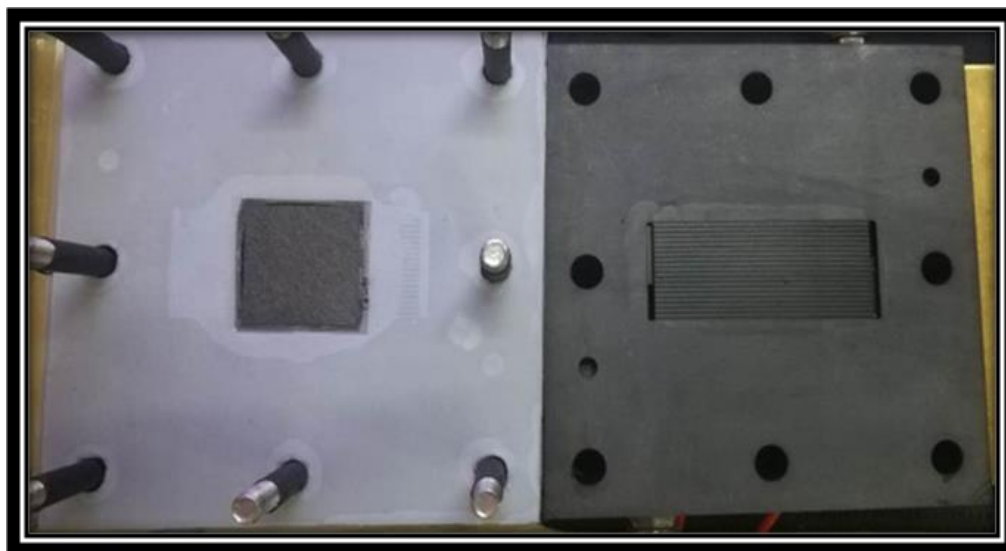


Figure 1. The single cell test device with parallel straight flow filed.

Table 1. The fuel cell configurations during the experiments.

Configuration	#1	#2	#3	#4	Switch#1	Switch#2	Switch#3	Switch#4
Active area	4cm <sup>2</sup>				4cm <sup>2</sup>			
Flow fields	20 channels(0.5 *0.5mm <sup>2</sup> )-machined graphite plate							
CCM	Anode:0.1mg·cm <sup>-2</sup> /Cathode: 0.4mg·cm <sup>-2</sup>				Anode:0.4mg·cm <sup>-2</sup> /Cathode: 0.1mg·cm <sup>-2</sup>			
Compression of GDL	20%							
Anode GDL with PTFE loads	20 wt.%	20 wt.%	20 wt.%	20 wt.%	0 wt.%	10 wt.%	20 wt.%	30 wt.%
Cathode GDL with PTFE loads	0 wt.%	10 wt.%	20 wt.%	30 wt.%	20 wt.%	20 wt.%	20 wt.%	20 wt.%

Polarization curves were measured in a single cell with an area of 4 cm<sup>2</sup>. And the bipolar plates were graphite with parallel flow patterns as shown in Figure 1. In order to minimize the effects of pressure drop and gas flow distribution on the mass transfer of oxygen, the flow field consisted of 20 parallel channels with a channel and land width of 0.5mm and a channel depth of 0.5 mm. The compressibility of MEAs were controlled at 20% based on the calculation method of Ref [39]. The polarization curves were measured by the HTS-125 fuel cell test station (HEPHAS, Scribner Associates 890e Fuel Cell Test System). Details configurations of fuel cell were shown in Table 1.

#### 2.4 Experimental procedure

Prior to the fuel cell test, each cell was conditioned by a step voltage at 65 ° C, 150 kPa<sub>abs</sub> and fully humidified hydrogen and air, in the following order: 0.6 V for 45 minutes, 0.45 V for 10 minutes and 0.85 V 5 minutes, repeat 8 times. For the measurement of the limiting current density, high flow rates of 1000 nccm H<sub>2</sub> on the anode and 3000 nccm (normal cubic centimes per minute; volumetric flow rate normalized to 273 K and 1 atm) diluted oxygen in various dry mole fraction (*x*O<sub>2</sub>, dry) between 1 % and 24 % on the cathode side are applied. This corresponds to high stoichiometry of >7 for both reactants at all measurement conditions. The cell was adjusted to the following conditions: cell temperature of 30°C to 80 °C, inlet pressure (*p*<sub>abs</sub>) of 100-300 kPa, and relative humidity (*RH*) of 70 % on anode and cathode side. High stoichiometry and a low pressure drop of <15 kPa minimized concentration and *RH* gradients between inlet and outlet of the flow field. For each cathode gas mixture, a polarization curve with proper constant current operate model until the voltage drop to <0.1V was recorded. Each current was held for 2 min at steady state prior to recording the data point (average of 15 sec). The limiting current *I*<sub>Lim</sub> was extracted from the polarization curve fitting results by FCView software (Scribner Associate, Inc.) through the equation as follows:

$$V = E_{theor} + b \cdot \log(i_0) - b \cdot \log(i) - i \cdot R_{ohm} + C_C \cdot \log\left(\frac{I_{Lim} - i}{I_{Lim}}\right) \quad (1)$$

The simplified empirical model used in FCView was based on the Butler-Volmer kinetics and mass transport effects as described by Bard and Faulkner [40]. Here, *E*<sub>theor</sub> is the theoretical (or reversible) potential and *i*<sub>0</sub> is the exchange current density, and *b* is the Tafel slope. The *R*<sub>ohm</sub> parameter is the ohmic resistance of a cell. *C* and *I*<sub>Lim</sub> are an empirical description of a mass transport limiting condition.

#### 2.5 The oxygen transport characterization with limiting current theory

While the transport of reactant gases in the fuel cell occurs by both diffusion and convection, transport towards the active catalyst site is primarily limited by diffusion process. Fick's law of diffusion can describe steady-state diffusion flux (*J*) of a species

$$J = -D \frac{\partial C}{\partial x} \quad (2)$$

Where *J* represents the amount transported per area and time, *D* is a diffusion coefficient and *C* is the concentration of the diffusing species, and *x* is the length coordinate. Assuming that the diffusion

coefficient is independent of concentration, which results in a linear concentration profile and  $J$ , simplifies to

$$J = D \frac{\Delta C}{L} \quad (3)$$

Where  $L$  is the diffused distance or diffusion path length and  $\Delta C$  is the positive concentration difference. The ratio of  $D/L$  is commonly referred to as the mass-transport coefficient,  $k$ , and the inverse of  $k$  can be defined as the mass transport resistance ( $R_{MT}$ ), so that

$$J = k\Delta C = \frac{\Delta C}{R_{MT}} \quad (4)$$

Because the molar flux of oxygen  $J_{O_2}$  is related to the current density  $i$  by the Faraday constant  $F$ , the total oxygen transport resistance ( $R_T$ ) may be expressed by

$$R_T = \frac{\Delta C_{O_2}}{J_{O_2}} = \frac{4F}{i} \Delta C_{O_2} \quad (5)$$

Where  $\Delta C_{O_2}$  is the change in oxygen concentration from the channel inlet to the electrode [41, 42]. When the cell operates at limiting current ( $I_{Lim}$ ), the oxygen concentration at the electrode approaches zero, and so the concentration difference  $\Delta C_{O_2}$  is simply equal to the inlet concentration ( $C_{O_2}^{inlet}$ ).  $C_{O_2}^{inlet}$  is related to the regulated dry mole fraction of oxygen ( $X_{O_2}^{inlet}$ ) by

$$\Delta C_{O_2} = C_{O_2}^{inlet} = \frac{P-P_W}{RT} X_{O_2}^{inlet} \quad (6)$$

The oxygen molecules have to travel through the bulk gas in the flow channel, through the open pores of the GDL and the CL. Each of the individual steps has its own mass-transport resistance and  $R_T$  could be represented by

$$R_T = \frac{4F}{I_{Lim}} \frac{P-P_W}{RT} X_{O_2}^{inlet} \quad (7)$$

The oxygen molecules have to travel through the bulk gas in the flow channel, through the open pores of the GDL and the CL. Each of the individual steps has its own mass-transport resistance and  $R_T$  could be represented by

$$R_T = R_{CH} + R_{GDL} + R_{CL} \quad (8)$$

$R_{CH}$  is described as the oxygen transport resistance in the flow field. The special designed flow filed reduces the pressure drop across the reaction region. With the minimized contribution from the gas channel,  $R_{CH}$  can be ignored in this work [43, 44]. The  $R_{GDL}$  and the  $R_{CL}$  are the oxygen transport resistance in the GDL and CL, respectively. GDL consist of substrate and MPL and  $R_{GDL}$  may be represented by

$$R_{GDL} = R_S + R_{MPL} \quad (9)$$

Considering pore size factor, the  $R_S$  is the molecular diffusion, which is in proportion to the pressure. But  $R_{MPL}$  and  $R_{CL}$  is mainly consist of Knudsen diffusion, which is independent with pressure [35, 37, 45]. So the  $R_T$  in this work also be expressed as

$$R_T = R_P + R_{NP} = (R_{GDL} + R_{MPL, Fick}) + (R_{MPL, Knudsen} + R_{CL, Knudsen}) + R_{CL, other} \quad (10)$$

Where  $R_P$  represents the pressure dependent oxygen transport resistance in carbon paper or cloth substrate open pores and the crack of MPL.  $R_{NP}$  represents the pressure independent oxygen flux resistance in MPL and CL micro pores (<50nm). Moreover,  $R_{CL, other}$  in CL may related to the local oxygen transport around the catalyst which refer to the diffusion in the ionomer film or water film [46]. The  $R_{NP}$  is related to the slope and intercept of the  $R_T$ - $P$  plot as described in Ref [45].

### 3. RESULTS AND DISCUSSION

#### 3.1 The performance of MEAs with various PTFE loading GDLs

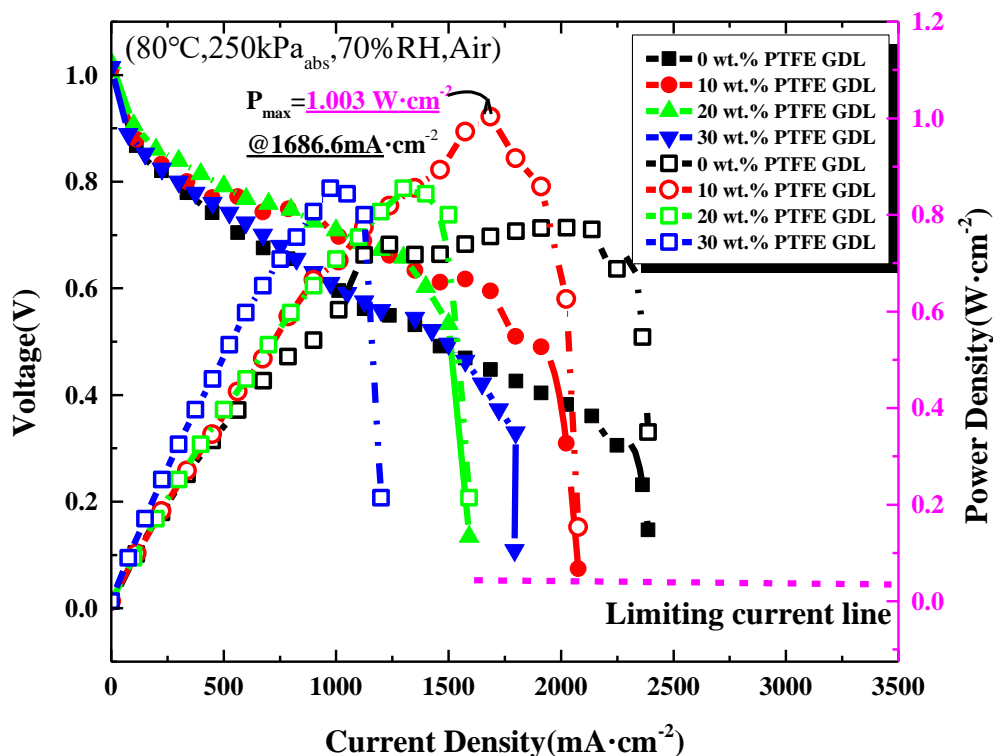


**Figure 2.** The performance of MEAs with various PTFE loading GDLs at  $0.4 \text{ mg}\cdot\text{cm}^{-2}$  Pt loading cathode testing at  $80^\circ\text{C}$ ,  $250\text{kPa}_{\text{abs}}$ ,  $70\% \text{RH}$  and cathode gas using air with high flow rates of  $1000 \text{ nccm H}_2$  on the anode and  $3000 \text{ nccm air}$  on cathode.

As reported in several publications [3, 8, 38, 47-49], the loading of PTFE had a crucial influence on the performance of fuel cell especially at high current densities. Figure 2 depicts the MEA performance with different PTFE contents in GDLs. There is a significant discrepancy in performance under high current density. The GDL in cathode side without PTFE coating shows a largest limiting current but minimal power density  $P_{\text{max}}$ . The cell with 10 wt. % PTFE coated GDL has the power density of  $1.003 \text{ W}\cdot\text{cm}^{-2}$  under  $1686.6 \text{ mA}\cdot\text{cm}^{-2}$ . Comparing the high PTFE loading, the one with a loading of 30 wt. % suffers a serious mass transport loss operating at high current region. The result is different with the report of Mukundan [29] where the best performance was under a PTFE loading of 20 wt. % but the area of the fuel cell was  $50 \text{ cm}^2$ . Maslan and Prasanna have reported a same result that the fuel cell with a PTFE loading lower than 20 wt. % would have a better performance and water permeability [8, 22]. Moreover, the GDL with a PTFE loading of 20 wt. % showed the lowest limiting current comparing to others. The similar conclusions could be found in the work of Biesdorf et al [3] where the used carbon paper was SGL carbon groups series 24 and the loading of PTFE in MPL was 23 wt.%. Thus, we can conclude that the optimal PTFE load of GDL is in the range of 5 to 10 wt. %.

And without PTFE in GDLs may increase the activation loss comparing the voltage drop before  $0.3 \text{ A}\cdot\text{cm}^{-2}$ .

### 3.2 The morphology of GDLs

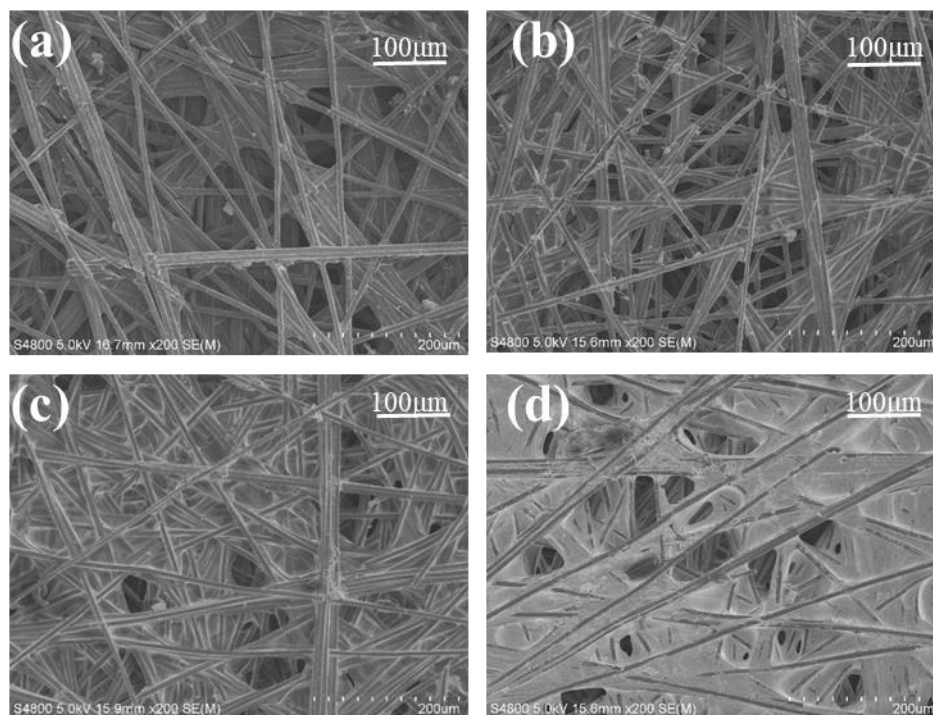


**Figure 3.** The SEM images of the different PTFE loading in GDLs (a): 0 wt. %; (b):10 wt. %; (c):20 wt. %; (d):30 wt. %.

The surface morphology of fresh GDL with different PTFE loading are shown in Figure 3. The pore size distribution was not uniform in the GDL without PTFE coating in Figure 3(a) and possessed many small pores and large pores. Increasing the loading of PTFE to 10.wt % in GDL, the pore size became uniform and the pores at the through plane could be observed clearly in Figure 3(b). When the loading of PTFE in GDL was much more than 20 wt. %, the small pores could be filled preferentially by PTFE and the space between the multiple intersecting graphite's fibers in Figure 3(d) was occupied. However, there were still some large pores in the GDL. This result has also been reported in literatures Ref [2, 22, 25].

### 3.3 The impact of temperatures on $R_T$ with various loading of PTFE coated in GDLs

The oxygen transport can be characterized by oxygen transport resistance  $R_T$  through limiting current method. However, there are many variables in experiments such as different diluted oxygen and the change of backpressure [35, 37, 43, 44, 50]. Moreover, the operating temperature may affect oxygen transport in the through plane direction [44]. However, most researches ignored the water effect in real operation. Shen et al.[51] reported that water behaviors was closely connected with

operating conditions which might rise the  $R_T$  nearby the catalyst through exploring the local  $O_2$  transport. In this paper, the impact of operating temperatures on  $R_T$  with various PTFE loading coated GDLs were investigated as shown in Figure 4. Various oxygen concentration of 1%, 2%, 3% and 4% and different operating temperatures of 30 °C ,40 °C , 50 °C , 60 °C , 70 °C and 80 °C were applied to test the  $I_{Lim}$  under different absolute pressure as 100kPa, 150kPa, 200kPa, 250kPa and 300kPa. Then, the  $R_T$  was calculated by equation (7) where the extremely low concentration oxygen gas and unsaturated RH conditions were considered to eliminating liquid water interference [37, 44].

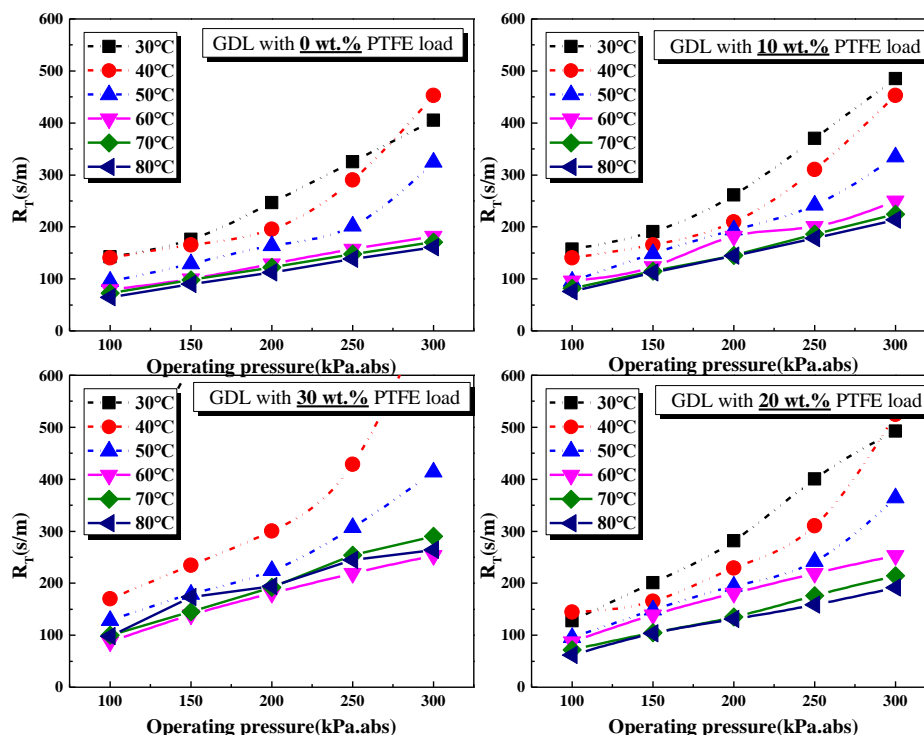


**Figure 4.** The change of oxygen transport resistance  $R_T$  with various PTFE load on cathode GDL at different operating temperatures (evaluated at low oxygen concentrations as 1%, 2%, 3% and 4%).

Theoretically, the  $R_T$  will increase linearly with increasing pressure and the slope of this line represents the gas diffusion ability of GDL, which obeys the Fick’s law and is pressure dependent. However, the  $R_T$  did not lineally increase when the cells operated at 30 °C, 40 °C, and 50 °C as show in Figure 4. The  $R_T$  increased sharply when the cells operate at the higher pressure of 200kPa, 250kPa and 300kPa. Comparing the four different PTFE loading GDLs, it was found that the  $R_T$  of single cell with 30 wt. % PTFE loading in GDL was more sensitive to the operating temperature. It is hard to dissect which component in MEA lead to such change. However, it still has an evidence showed that the water was easily condensed at the low temperatures and the high pressures [51]. That might be the reason that the temperature higher than 50°C was chosen to investigate the  $R_T$  by most researchers [45, 51-54]. Based on the above observation, we can conclude that the higher temperature ( $\geq 60$  °C) will be

more proper to characterize the oxygen transport resistance through limiting current method, especially for the characterization of the oxygen diffusion with pressure independent ( $R_{NP}$ ).

3.4 The impact of PTFE loading in GDLs on  $R_{NP}$  at  $0.4\text{mg}\cdot\text{cm}^{-2}$  Pt loading cathode

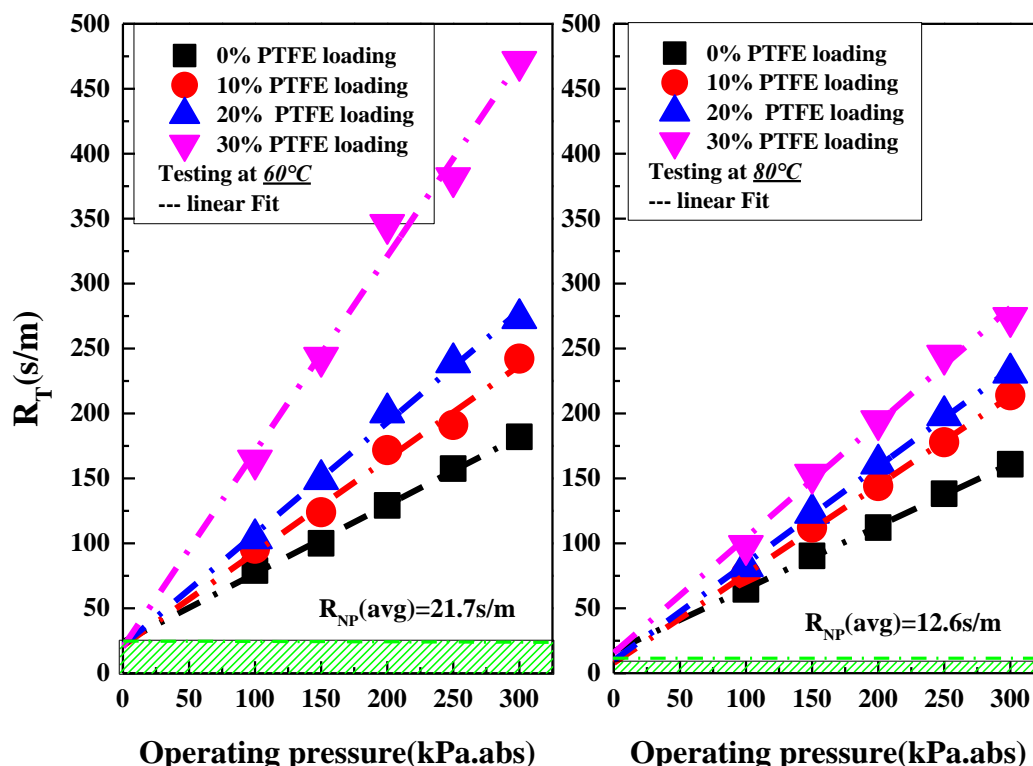


**Figure 5.** The impact of PTFE loading in GDLs on  $R_T$  and  $R_{NP}$  when fuel cell operating at 60°C and 80°C. (The shaded area represents the average value of  $R_{NP}$ )

Based on the above statement, the  $R_{NP}$  in MEAs with various PTFE loading in GDLs were measured under operating temperature of 60°C and 80 °C have shown in Figure 5. The intercept of the  $R_T$ -P plot represents the  $R_{NP}$ . Since the same MPL and CL were applied on the MEAs, the  $R_{NP}$  could be considered as the constant value. Thus, the average value of  $R_{NP}$  could be obtained from Figure 5 respectively as 21.7 s/m at 60 °C and 12.6 s/m at 80 °C. As expected, the operating temperature was benefited for oxygen diffusion in cells. It is similar to the report by Nonoyama et al [44]. And the deviation compared to the literatures might be due to the different humidification and various CLs used in MEAs [44, 55]. Compared to the slope of the  $R_T$ -P plot in Figure 5, the GDL with high PTFE load, the slope would be large and the oxygen diffusion ability of GDL would be reduced, which indicated that the PTFE coated in GDL was not benefit for the oxygen transport in the cathode. However, these results were only suitable for mass transfer of oxygen through the un-wetting GDLs. Additionally, the  $R_T$ -P plot could be used as a novel method to in-suit characterize the gas diffusion property of dry and compressed GDLs.

3.5 The impact of PTFE loading in GDLs on  $R_{NP}$  at low Pt loading as  $0.1\text{mg}\cdot\text{cm}^{-2}$

In order to verify the in-suit characterization method of GDLs under dry and compressed situation, the  $R_T$ -P plots of the switched cells which had exchanged the GDLs of the anode and cathode were built as shown in Figure 6. Then the switched cells had the same GDL as the PTFE loading was 20 wt. % in cathode and altered the PTFE loading in anode GDL. Specially, the Pt loading of cathode was  $0.1\text{mg}\cdot\text{cm}^{-2}$ .

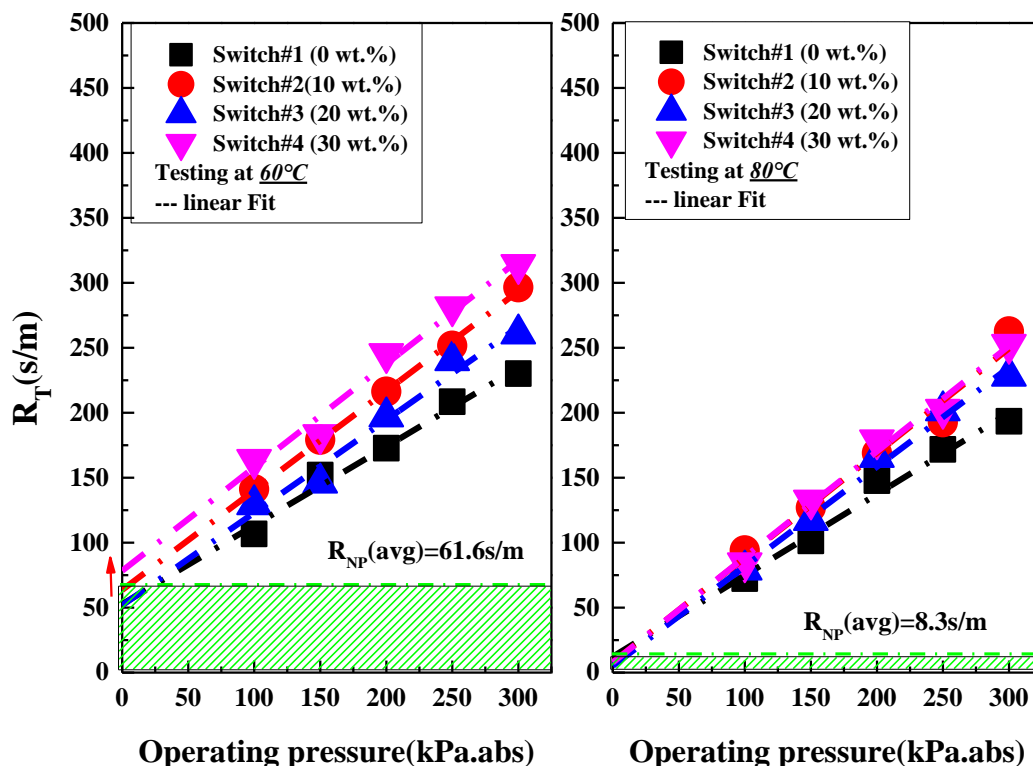


**Figure 6.** The impact of PTFE loading in GDLs on  $R_T$  and  $R_{NP}$  when fuel cell operating at  $60^\circ\text{C}$  and  $80^\circ\text{C}$  while the original anode was switched to be using as the cathode. (The shaded area represents the average value of  $R_{NP}$ )

The parallel fitting lines are displayed in Figure 6, which represents the same slope of the GDLs. Compared the slope with 20wt. % loading one in Figure 5, it had the approximate values of 0.86 at  $60^\circ\text{C}$  and 0.74 at  $80^\circ\text{C}$ . The slightly difference of the slop in Figure 6 at  $80^\circ\text{C}$  could be explained by the deviation of compression during assembling the cells. Nevertheless, the good linear relationship in Figure 6 at  $60^\circ\text{C}$  showed the applicability of this method.

For the  $R_{NP}$  in Figure 6 testing at  $60^\circ\text{C}$ , it increased twice more than the one in Figure 5. Interestingly, increasing PTFE loading in GDL used as the anode in the switched cell, the  $R_{NP}$  also had a trend of increase. However, for the  $R_{NP}$  in Figure 6 tested at  $80^\circ\text{C}$ , the change was not obvious. This phenomenon could not be found in any other literatures. It could be inferred that the PTFE loading increased in GDL of anode would decrease thermal conductivity resulted in accumulating liquid water in cathode CLs [50]. The increase of average value of  $R_{NP}$  could be due to the local  $\text{O}_2$  transport resistance increased in the low Pt loading [44]. With the temperature increased to  $80^\circ\text{C}$ , the change of

average value of  $R_{NP}$  was small. Meanwhile, the effect of loading of PTFE coated in GDL in anode has not been explored before. Therefore, it has the reason to suspect that there was the less condensed liquid water in the low Pt loading CLs when operated at high temperature [3, 51, 56].

3.6 The pore size distribution and the calculation of in-suit effective diffusion coefficient of various PTFE loading in GDLs

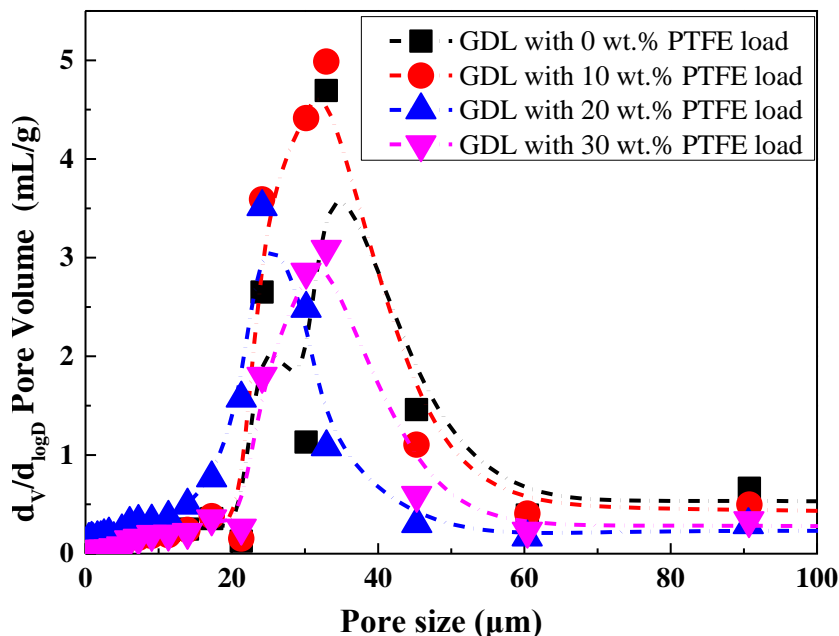


Figure 7. The pore size distribution of various PTFE loading GDLs.

Figure 7 displays the pore size distribution of GDLs with various PTFE loading. It shows that the 10 wt. % PTFE loading had the best pore size distribution compared to others. GDL without PTFE coating had two peaks which corresponded to the small and large pores in the image shown in Figure 2(a). Moreover, the porosity and tortuosity data could be obtained through mercury intrusion porosimetry as shown in Table 2. As expected that the tortuosity increased with increasing PTFE loading, but not the porosity.

Table 2. The gas diffusion parameter of different PTFE load GDLs.

Diffusion Parameter	Porosity ( $\epsilon$ )	Tortuosity ( $\tau$ )
0 wt.%	62.42%	2.795
10 wt.%	62.07%	2.8893
20 wt.%	60.85%	3.2862
30 wt.%	62.62%	3.4439

As popular known that, the oxygen effective diffusion coefficient  $D_{eff}$  for porous materials is related with the porosity  $\epsilon$  and tortuosity  $\tau$  as follow

$$D_{eff} = \frac{\epsilon}{\tau} D_{O_2,mix} \quad (11)$$

Where the  $D_{O_2,mix}$  represents the diffusional properties of multicomponent gases which is linear with  $1/P$ . In this investigation, the gas specials and operating temperatures were fixed. Then, the constant value  $\alpha$  can be obtained through calculation [57].

Considering the compression ratio  $\sigma$ , the equation (11) can be expressed as

$$D_{real} = \sigma \times \frac{\epsilon}{\tau} \times \alpha \times \frac{1}{P} \quad (12)$$

Similarly, the real in-suit diffusion coefficient  $D_{real}$  is the derivative of  $R_P$  and is pressure dependent.

$$D_{real} = \frac{1}{R_P} = \frac{1}{b \cdot P} \quad (13)$$

Thus, the slop  $b$  in the  $R_T$ - $P$  plot can be calculated by

$$b = \alpha \cdot \frac{\tau}{\epsilon} \quad (14)$$

Where,  $\alpha$  is still the constant value in when the operating conditions and configuration of cells are fixed in testing. Through the calculation by equation (12) and equation (13), it shows good consistent results. Therefore, the limiting current method has the advantage to characterize the real in-suit diffusion coefficient of GDLs.

### 3.7 The analysis of water behaviors in various PTFE loading GDLs

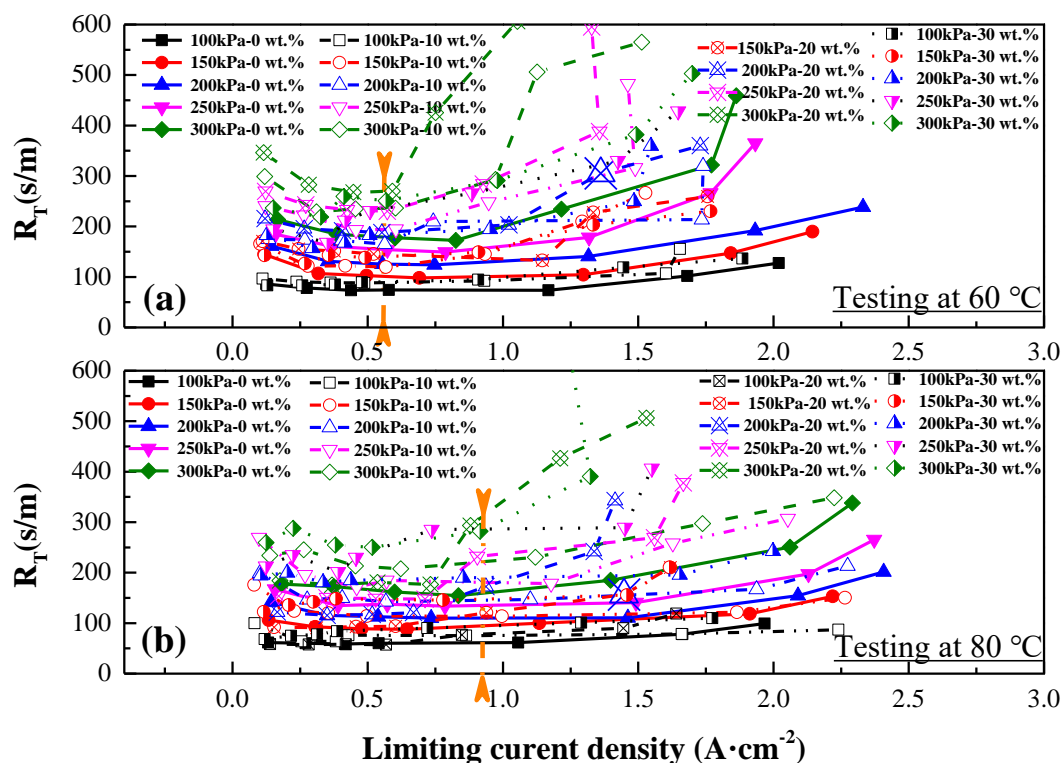


**Figure 8.** The water behaviors affect by  $R_T$  under different temperature and pressure with cathode Pt loading as  $0.4\text{mg}\cdot\text{cm}^{-2}$ : (a)  $60\text{ }^\circ\text{C}$ ; (b)  $80\text{ }^\circ\text{C}$ .

The computed  $R_T$  in various PTFE loading with Pt loading of  $0.4\text{mg}\cdot\text{cm}^{-2}$  in cathode CL are displayed in Figure 8 as a function of limiting current. Following the definition made by Caulk et al [50], the  $R_T$  in Figure 8 could be divided into two distinct regions: “dry region” and “transition region”, where  $R_T$  is independent of limiting current, followed by a dry-to-wet transition. Obviously, the dry region became widely at high operating temperature of  $80^\circ\text{C}$ . Similar results has been reported by Lu et al [45],  $R_T$  increased rapidly with limiting current in the transition region. The increase of  $R_T$  with limiting current was more significant at high gas pressure. This phenomenon was more obvious at an operating temperature of  $60^\circ\text{C}$ .

Compared the cells with different PTFE loading in GDLs, the ones with a low loading had the wider transition region, which was more signification when the cells were operated at high pressure and low temperature. Operated under low pressure and high temperature conditions, there had no too much change in the dry region which showed that the GDLs were always in dry state. The water behaviors analyses showed that GDLs coated with PTFE were easier to become wet than the ones without PTFE especially at poor operating conditions. Moreover, too much PTFE in GDLs could change the distribution of water when PEMFC was operated at high current density. Biesdorf et al [3] reported that high mass transport losses did not always correlate with high amount of water but the water distribution. And the optimal PTFE loading in GDLs was between 5 wt. % and 10 wt. % for high performance PEMFC which was consistent with our result.

#### 4. CONCLUSIONS

The oxygen transport and water behaviors of PEMFC with different PTFE contents in GDL are studies by limiting current method. Special flow field with narrow channel and high stoichiometric ratio are applied for minimizing the pressure drop and the gas diffusion loss under rib. Fuel cell with a PTFE loading in GDL of 10wt. % has the best performance of  $1.003\text{ W}\cdot\text{cm}^{-2}$ . The SEM morphology shows that the PTFE will change the pore structures and distribution of GDLs. The GDLs with a PTFE loading of 10wt. % has the most uniform pore distribution. Tested  $R_T$  under various temperatures show that the water more easily accumulates at lower temperature which will disturb the leaner relationship of  $R_T$ -P. Therefore, the high temperature ( $\geq 60^\circ\text{C}$ ) will be properly applied to characterize the oxygen transport through limiting current method, especially for the characterization of the oxygen diffusion with pressure independent. The slope of  $R_T$ -P plot can be used to evaluate the in-suit oxygen transport ability of dry and compressed GDL. The GDL without PTFE has the best oxygen transport ability at dry state. The different PTFE loading in GDLs used in anode has the effect on the  $R_{NP}$  especially with the low Pt loading, which is suspected by the liquid water formation at the cathode CLs or MPLs. The water behaviors analyses show that the GDLs coated with PTFE are more easily to be wet than the ones without PTFE especially at poor operating conditions.

#### ACKNOWLEDGEMENTS

This work will thank to support of National Key Research and Development Program of China (No. 2016YFB0101205), Hubei Province Technology Innovation Project (Program No. 2016AAA047)

**References**

1. D. Banham, S. Ye, *ACS Energy Lett.*, 2 (2017) 629.
2. C. Lim, C.Y. Wang, *Electrochim. Acta*, 49 (2004) 4149.
3. J. Biesdorf, A. Forner-Cuenca, T.J. Schmidt, P. Boillat, *J. Electrochem. Soc.*, 162 (2015) F1243.
4. J. Biesdorf, P. Oberholzer, T.J. Schmidt, P. Boillat, *ECS Trans.*, 64 (2014) 467.
5. G.R. Molaeimanesh, M.H. Akbari, *Int. J. Hydrogen Energy*, 39 (2014) 8401.
6. M. Mortazavi, K. Tajiri, *J. Power Sources*, 245 (2014) 236.
7. L. Hao, P. Cheng, *Int. J. Heat Mass Transfer*, 55 (2012) 133.
8. H. Sadeghifar, N. Djilali, M. Bahrami, *J. Power Sources*, 248 (2014) 632.
9. N.H. Maslan, M.M. Gau, M.S. Masdar, M.I. Rosli, *J. Nat. Gas Sci. Eng.*, 11 (2016) 85.
10. R. Kuwertz, N. Aoun, T. Turek, U. Kunz, *J. Electrochem. Soc.*, 163 (2016) F988.
11. S. Kim, B.-H. Jeong, B.K. Hong, T.-S. Kim, *J. Power Sources*, 270 (2014) 342.
12. N. Khajeh-Hosseini-Dalasm, T. Sasabe, T. Tokumasu, U. Pasaogullari, *J. Power Sources*, 266 (2014) 213.
13. T.V. Reshetenko, J. St-Pierre, K. Artyushkova, R. Rocheleau, P. Atanassov, G. Bender, M. Ulsh, *J. Electrochem. Soc.*, 160 (2013) F1305.
14. R. Vijay, S.K. Seshadri, P. Haridoss, *T. Indian. I. Metals*, 64 (2011) 175.
15. H.-M. Chang, C.-W. Lin, M.-H. Chang, H.-R. Shiu, W.-C. Chang, F.-H. Tsau, *J. Power Sources*, 196 (2011) 3773.
16. M.S. Ismail, T. Damjanovic, K. Hughes, D.B. Ingham, L. Ma, M. Pourkashanian, M. Rosli, *J. Fuel Cell Sci. Tech.*, 7 (2010) 051016.
17. J.-H. Lin, W.-H. Chen, Y.-J. Su, T.-H. Ko, *Energ. Fuel*, 22 (2008) 1200.
18. G. Velayutham, J. Kaushik, N. Rajalakshmi, K.S. Dhathathreyan, *Fuel Cells*, 7 (2007) 314.
19. J.T. Gostick, M.W. Fowler, M.A. Ioannidis, M.D. Pritzker, Y.M. Volfkovich, A. Sakars, *J. Power Sources*, 156 (2006) 375.
20. G. Lin, T.V. Nguyen, *J. Electrochem. Soc.*, 152 (2005) A1942.
21. L. Giorgi, E. Antolini, A. Pozio, E. Passalacqua, *Electrochim. Acta*, 43 (1998) 3675.
22. M. Prasanna, H.Y. Ha, E.A. Cho, S.A. Hong, I.H. Oh, *J. Power Sources*, 131 (2004) 147.
23. G.-G. Park, Y.-J. Sohn, T.-H. Yang, Y.-G. Yoon, W.-Y. Lee, C.-S. Kim, *J. Power Sources*, 131 (2004) 182.
24. S. Park, B.N. Popov, *Fuel*, 88 (2009) 2068.
25. S. Park, J.-W. Lee, B.N. Popov, *J. Power Sources*, 177 (2008) 457.
26. J.M. Lamanna, S.G. Kandlikar, *Int. J. Hydrogen Energy*, 36 (2011) 5021.
27. J. Lobato, P. Cañizares, M.A. Rodrigo, C. Ruiz-López, J.J. Linares, *J. Appl. Electrochem.*, 38 (2008) 793.
28. S. Park, J.-W. Lee, B.N. Popov, *Int. J. Hydrogen Energy*, 37 (2012) 5850.
29. A.K.M.F. Mathias, *J. Phys. Chem. Lett.*, (2016).
30. R. Mukundan, J.R. Davey, T. Rockward, J.S. Spendelow, B. Pivovar, D.S. Hussey, D.L. Jacobson, M. Arif, R. Borup, *ECS Trans.*, 11 (2007) 411.
31. C.-J. Tseng, S.-K. Lo, *Energ. Convers. Manage.*, 51 (2010) 677.
32. A. Forner-Cuenca, V. Manzi-Orezzoli, J. Biesdorf, M.E. Kazzi, D. Streich, L. Gubler, T.J. Schmidt, P. Boillat, *J. Electrochem. Soc.*, 163 (2016) F788.
33. A. Forner-Cuenca, J. Biesdorf, V. Manzi-Orezzoli, L. Gubler, T.J. Schmidt, P. Boillat, *J. Electrochem. Soc.*, 163 (2016) F1389.
34. A. Forner-Cuenca, J. Biesdorf, A. Lamibrac, V. Manzi-Orezzoli, F.N. Büchi, L. Gubler, T.J. Schmidt, P. Boillat, *J. Electrochem. Soc.*, 163 (2016) F1038.
35. A. Forner-Cuenca, In, *Eth Zürich*, 2016.
36. D.R. Baker, D. Caulk, A. Chuang, *Meeting Abstracts*, Ma2010-02 (2010) 889.
37. D.A. Caulk, D.R. Baker, *J. Electrochem. Soc.*, 158 (2011) B384.

38. D.R. Baker, D.A. Caulk, *ECS Trans.*, 50 (2013) 35.
39. S.M. Moosavi, M. Niffeler, J. Gostick, S. Haussener, *Chem. Eng. Sci.*, 176 (2018) 503.
40. C. Simon, F. Hasché, H.A. Gasteiger, *J. Electrochem. Soc.*, 164 (2017) F591.
41. L.L Faulkner, A.J Bard. *Electrochemical Methods: Principles and Applications*, (2001) 386-428.
42. D.R. Baker, C. Wieser, K.C. Neyerlin, M.W. Murphy, *ECS Trans.*, 3 (2006) 989.
43. D.R. Baker, D.A. Caulk, K.C. Neyerlin, M.W. Murphy, *J. Electrochem. Soc.*, 156 (2009) B991.
44. T. Mashio, A. Ohma, S. Yamamoto, K. Shinohara, *ECS Trans.*, 11 (2007) 529.
45. N. Nonoyama, S. Okazaki, A.Z. Weber, Y. Ikogi, T. Yoshida, *J. Electrochem. Soc.*, 158 (2011) B416.
46. Z. Lu, J. Waldecker, M. Tam, M. Cimenti, *ECS Trans.*, 69 (2015) 1341.
47. A.Z. Weber, A. Kusoglu, *J. Mater. Chem. A.*, 2 2 (014) 17207.
48. R. Omrani, B. Shabani, *Int. J. Hydrogen Energy*, 42 (2017) 28515.
49. D.M. Fadzillah, M.I. Rosli, M.Z.M. Talib, S.K. Kamarudin, W.R.W. Daud, *Renew. Sust. Energ. Rev.*, 77 (2017) 1001.
50. F. Lopicque, M. Belhadj, C. Bonnet, J. Pauchet, Y. Thomas, *J. Power Sources* , 336 (2016) 40.
51. D.A. Caulk, D.R. Baker, *J. Electrochem. Soc.*, 157 (2010) B1237.
52. S. Shen, X. Cheng, C. Wang, X. Yan, C. Ke, J. Yin, J. Zhang, *Phys. chem. chem. phys.*, (2017).
53. J.P. Owejan, T.A. Trabold, M.M. Mench, *Int. J. Heat Mass Transfer*, 71 (2014) 585.
54. T.V. Reshetenko, J. St-Pierre, *J. Power Sources*, 161 (2014) F1089.
55. H. Oh, Y.I. Lee, G. Lee, K. Min, J.S. Yi, *J. Power Sources*, 345 (2017) 67.
56. K.C. Neyerlin, J.M. Christ, J.W. Zack, W. Gu, S. Kumaraguru, A. Kongkanand, S.S. Kocha, *Meeting Abstracts*, Ma2016-02 (2016) 2492.
57. S.-W.C. Ryan O'hayre, Whitney Colella, Fritz B. Prinz, *Engineering & Materials Science / Mechanical Engineering / Thermodynamics*, (January 2009) 576 Pages.

© 2018 The Authors. Published by ESG ([www.electrochemsci.org](http://www.electrochemsci.org)). This article is an open access article distributed under the terms and conditions of the Creative Commons Attribution license (<http://creativecommons.org/licenses/by/4.0/>).